International Journal of Modern Engineering Research (IJMER)
www.ijmer.com Vol.2, Issue.2, Mar-Apr 2012 pp-186-196 ISSN: 2249-6645

A Novel of Bidirectional DC-DC converter drive

N.MAHESH
M-Tech Scholar, Power Electronics and Drives,
Department Of Electrical And Electrical Engineering,
Koneru Lakshmaiah University, Guntur,(A.P), India.

D.SESHI REDDY
Associate professor,
Department Of Electrical And Electrical Engineering,
Koneru Lakshmaiah University, Guntur,(A.P),India.

Abstract: - A Novel of bidirectional DC-DC converter drive is presented in this paper. The circuit configuration of the proposed converter is very simple. The proposed converter employs a coupled inductor with same winding turns in the primary and secondary sides. In step-up mode, the primary and secondary windings of the coupled inductor are operated in parallel charge and series discharge to achieve high step-up voltage gain. In step-down mode, the primary and secondary windings of the coupled inductor are operated in series charge and parallel discharge to achieve high step-down voltage gain. Thus, the proposed converter has higher step-up and step-down voltage gains than the conventional bidirectional DC-DC boost/buck converter. Under same electric specifications for the proposed converter and the conventional bidirectional boost / buck converter, the average value of the switch current in the proposed converter is less than the conventional bidirectional boost / buck converter. The operating principle and steady-state analysis are discussed in detail. Finally, a 70 / 210 V simulation circuit is simulated in MATLAB/Simulink to verify the performance for the automobile dual - battery drive system.

Index Terms: - Bidirectional DC-DC converter drive, coupled inductor.

I .Introduction

Bidirectional DC–DC converters are used to transfer the power between two DC sources in either direction. These converters are widely used in applications, such as hybrid electric vehicle energy systems [1]–[4], uninterrupted power supplies [5], [6], fuel-cell Hybrid power systems [7]–[10], PV hybrid power systems [11], [12] and battery chargers [13]–[15]. Many bidirectional DC-DC converters have been researched. The bidirectional DC-DC fly back converters are more attractive due to simple structure and easy control. However, these converters suffer from high voltage stresses on the power devices due to the leakage-inductor energy of the transformer. In order to recycle the leakage inductor energy and to minimize the voltage stress on the power devices, some literatures present the energy regeneration techniques to clamp the voltage stress on the power devices and to recycle the leakage-inductor energy, some literatures research the isolated bidirectional DC-DC converters, which include the half-bridge types and full-bridge types. These converters can provide high step-up and step-down voltage gainby adjusting the turn's ratio of the transformer. For non-isolated applications, the non-isolated bidirectional DC-DC converters, which include the conventional boost/buck types, multi-level type, three-level type, sepic/zeta type, switched-capacitor type, and coupled-inductor type, are presented. The multi-level type is a magnetic-less converter, but 12 switches are used in this converter. If higher step-up and step-down voltage gains are required, more switches are needed. This control circuit becomes more complicated. In the three-level type, the voltage stress across the switches on the three-level type is only half of the conventional type. However, the step-up and step-down voltage gains are low. Since the sepic/zeta type is combined of two power stages, the conversion efficiency will be decreased.

The development of bidirectional dc-dc converters has recently become increasingly important for clean-energy vehicle applications because battery-based energy storage systems are required for cold starting and battery recharging [16], [17], [18]. Bidirectional converters transfer power between two dc sources in both directions. However, back-up power from the battery is supplied using a bidirectional converter, which is employed in many uninterrupted power supplies (UPS), the front-end stage for clean-energy sources and dc motor driver circuits. The dc back-up energy system typically consists of numerous low-voltage-type batteries. Although a storage battery series string can provide high voltage, slight mismatches or temperature differences can cause a charge imbalance when the series string is charged as a unit Charge equalization cycles must be employed to correct this imbalance. However, conventional approaches to this process will stress the batteries, shorten their life and are limited to low-capacity power. Batteries arranged in parallel strings can enhance the power redundancy supplied by a battery and alleviate the problems caused by storage battery series strings. However, the output voltage remains low in this parallel connection configuration. A highly efficient bidirectional DC–DC converter with high-voltage diversity is a key component for batteries connected in parallel. Bidirectional DC - DC converters with transformer-based structures are the most common topologies. Soft switching techniques are generally applied to reduce the corresponding switching losses. These mechanisms with isolated transformers have high conduction losses because four to nine power switches are required. Many applications call for high-step-up converters that do not require isolation, such as the front-end converter with dual inputs. Accordingly, practical implementation is complex and costly. Switched-capacitor dc–dc converters have attracted much attention as an alternative method for providing bidirectional power flow control. However, increased switching loss and current stress are the critical drawbacks. The primary challenge is to design a circuit that has few switching devices and capacitors. Generally, the bidirectional converter in the UPS must generally boost 48–400 V, which is appropriate for eightfold step-up voltage gain. Zhao and Lee developed a family of highly efficient, high-step-up dc–dc converters by adding only one additional diode and a small capacitor [19]. This capacitor can recycle leaked energy and eliminate the reverse-recovery problem. In this approach the magnetic core can be regarded as a fly-back transformer and most energy is stored in the magnetic inductor.

1.1 COUPLED INDUCTOR:

The pair of coupled coils shown in figure has currents, voltages and polarity dots indicated. In order to show $M_{12} = M_{21}$ we begin by letting all currents and voltages are zero, thus establishing zero initial energy storage in the network. We then open –circuit the right–hand terminal pair and increase I_1 from zero to some constant value I_1 at time t = t_1.The power entering the network from left at any instant is

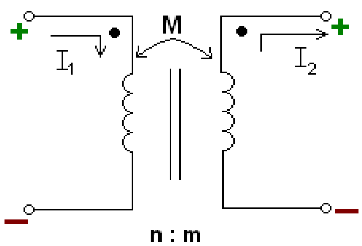

Fig 1 Coupled inductors

$$V_1 i_1 = L_1 \frac{di_1}{dt} i_1 \quad (1)$$

and the power entering from the right is

$$V_2 I_2 = 0 \quad (2)$$

Since i_2=0

The energy stored within the network when $i_1 = I_1$ is thus

$$\int_0^{t1} v1i1\, dt = \int_0^{I1} l1i1\, di1 = \frac{1}{2} L1I1^2 \quad (3)$$

We now hold I_1 constant, $i1 = I_1$, and let I_2 change from zero at t=t_1 to some constant value I_2 at t=t_2.The energy delivered from the right-hand source is thus

$$\int_{t1}^{t2} v2i2\, dt = \int_0^{I2} l2i2\, di2 = \frac{1}{2} L2i2^2 \quad (4)$$

However, even though the value of I_1 remains constant, the left-hand source also delivers energy to the network during this time interval

$$\int_{t1}^{t2} v1i1\, dt = \int_{t1}^{t2} M12 \frac{di2}{dt} i1dt = M12I1 \int_0^{I2} di2 = M12I1I2 \quad (5)$$

The total energy stored in the network when both i_1 and i_2 have reached constant values is

$$W_{total} = \frac{1}{2} L_1 I_1^2 + \frac{1}{2} L_2 I_2^2 + M_{12} I_1 I_2 \quad (6)$$

Now, we may establish the same final currents in this network by allowing the currents to reach final values to the reverse order

$$W_{total} = \frac{1}{2} L_1 I_1^2 + \frac{1}{2} L_2 I_2^2 + M_{21} I_1 I_2 \quad (7)$$

The only difference is the interchange of the mutual inductance M_{21} and M_{12}

$M_{12} = M_{21} = M$ and

$$W = \frac{1}{2} L_1 I_1^2 + \frac{1}{2} L_1 I_2^2 + M I_1 I_2 \quad (8)$$

If one current enters a dot-marked terminal while the other leaves a dot marked terminal

$$W = \frac{1}{2} L_1 I_1^2 + \frac{1}{2} L_1 I_2^2 - M I_1 I_2 \quad (9)$$

From equations 8 and 9 were derived final values of the two currents as constant, these “constants” can have any value and the energy expressions correctly represent the energy stored when the instantaneous values i_1 and i_2 are I_1 and I_1 respectively

$$W(t) \frac{1}{2} L_1 [i_1(t)]^2 + \frac{1}{2} L_2 [i_2(t)]^2 \pm M [i_1(t)] [i_2(t)] \quad (10)$$

1.1.1 The coupling coefficient

The degree to which M approaches its maximum value is described by the coupling coefficient, defined as

$$K = \frac{M}{\sqrt{L_1 L_2}} \quad (11)$$

Since $M \leq \sqrt{L_1 L_2}$

$$0 \leq k \leq 1$$

The larger values of the coefficient of coupling are obtained with coils which are physically closer, which are wound or oriented to provide a larger common magnetic flux, or provided with a common path through a material which serves to concentrate and localize the magnetic flux. Coils having a coefficient of coupling close to unity are said to be tightly coupled.

1.2 DC MACHINE: Back EMF induced in motor armature. When current passed through the armature of dc machines and its field coils excited torque is established and motor rotates the direction of rotation can be reversed by reversing either armature current or polarity of the magnets. Rotation of the armature gives rise to an induced emf which according to Lenz's law, will oppose the flow of current. Hence if

Ea=the numerical value of the induced emf.

Va=the numerical value of the applied voltage.

The armature currents is given by

$I_a = (V_a - E_a) / \tau_m$

$V_a = E_a + I_a \tau_m$

The power input $V_a I_a = E_a\ I_a + I_a^2 r_m$ (12)

The emf generated by the armature must have a perfectly definite value for particular value of the load current

$E_a = V_a - I_a\ r_m$ (13)

The induced emf is also determined from ordinary considerations of flux, number of conductors and speed, and its thus

$E_a = Z_e \times 2p\emptyset n$ (14)

From above 13 and 14 equations are equal we get

$V_a - I_a\ r_m = Z_e \times 2p\emptyset n$

$$n = \frac{V_a - I_a\, r_m}{Z_e \times 2p\emptyset n} \quad (15)$$

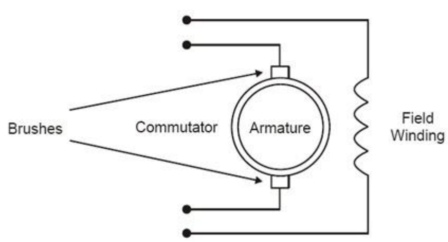

Fig 2 Dc motor basic parts

Hence the speed of dc motor may be controlled by

1. Varying the value of the flux.
2. Varying the value of the voltage applied to the motor armature
3. Varying the value of the effective number of conductors in series.

1.2.1 Field control:- In field control the applied armature voltage v is maintained constant. Then the speed is represented by equation as

$$\boldsymbol{\omega_m\ \alpha\ \frac{1}{I_f}} \quad (16)$$

1.2.2 Armature control:- In this the field current is maintained constant. Then the speed is derived from the equation as

$$\omega_m = (v - i_a R_a) \quad (17)$$

Hence, varying the applied voltage changes speed. Reversing the applied voltage changes the direction of rotation of the motor

1.2.3 Armature and Field control:- By combination armature and field control for speeds below and above the rated speed, respectively, a wide range of speed control is possible

$$T_e = K\emptyset_f i_a \quad (18)$$

Can be normalized if it is divided by rated torque

Which is expressed as

$$T_{er} = K\emptyset_{fr} i_{ar} \quad (19)$$

$$T_{en} = \frac{T_e}{T_{er}} = K\frac{\emptyset_f i_a}{K\emptyset_{fr} i_{ar}} = \emptyset_{fn} i_{an}, p.u. \quad (20)$$

Normalized eliminates machine constants, compacts the performance equation, and enables the visualization of performance characteristics regardless of machine size on same scale. the normalized torque, flux and armature current are

$$T_{en} = \frac{T_e}{T_{er}}, p. \quad (21)$$

$$\emptyset_{fn} = \frac{\emptyset_f}{\emptyset_{fr}}, \text{p.u} \quad (22)$$

$$i_{an} = \frac{i_a}{i_{ar}}, p.u \quad (23)$$

As the armature current is maintained at 1 p.u

$$T_{en} = \emptyset_{fn}, p.u \quad (24)$$

Hence normalized electromagnetic torque characteristics coincides with normalized field flux, similarly the air gap power is,

$$p_{an} = e_n i_{an}, p.u \tag{25}$$

Where e_n is the normalized induced emf.

As i_{an} is set to 1 p.u., the normalized air gap power becomes

$$p_{an} = e_n, p.u \tag{26}$$

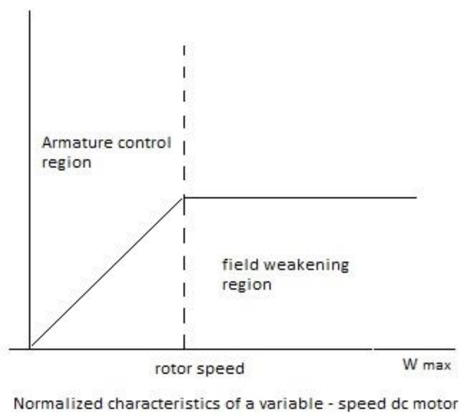

Fig 3 normalized characteristics of variable –speed DC motor

II. STEP–UP MODE

The proposed converter in step-up mode is shown in Fig 5. The pulse width modulation (PWM) technique is used to control the switches S_1 and S_2 simultaneously. The switch S_3 is the Synchronous rectifier.

2.1 CCM Operation

Mode 1: During this time interval, S_1 and S_2 are turned on and S_3 is turned off. The current flow path is shown in Fig 5(a). The energy of the low-voltage side V_L is transferred to the coupled inductor. Meanwhile, the primary and secondary windings of the coupled inductor are in parallel. The energy stored in the capacitor C_H is discharged to the load. Thus, the voltages across L_1 and L_2 are obtained as

$$u_{L1} = u_{L2} = V_L \tag{27}$$

By substituting above equations we get

$$\frac{di_{L1}(t)}{dt} = \frac{di_{L2}(t)}{dt} = \frac{V_L}{(1+k)L}, \tag{28}$$

Mode-2: During this time interval S_1 and S_2 are turned on and $S3$ is turned off. The current flow path is shown in Fig. 5(b). The energy of the low-voltage side V_L is transferred to the coupled inductor. Meanwhile, the primary and secondary windings of the coupled inductor are in parallel. The energy stored in the capacitor C_H is discharged to the load. Thus, the voltages across L_1 and L_2 are obtained as

$$i_{L1} = i_{L2}$$

$$u_{L1} + u_{L2} = V_L - V_H \tag{29}$$

By substituting above equations we get

$$\frac{di_{L1}(t)}{dt} = \frac{di_{L2}(t)}{dt} = \frac{V_L - V_H}{2(1+k)L}, \tag{30}$$

By using the state-space averaging method, the following equation is derived from

$$\frac{DV_L}{(1+k)L} + \frac{(1-D)(V_L - V_H)}{2(1+k)L} = 0 \tag{31}$$

By simplifying we get

$$G_{CCM(step-up)} = \frac{V_H}{V_L} = \frac{1+D}{1-D} \tag{32}$$

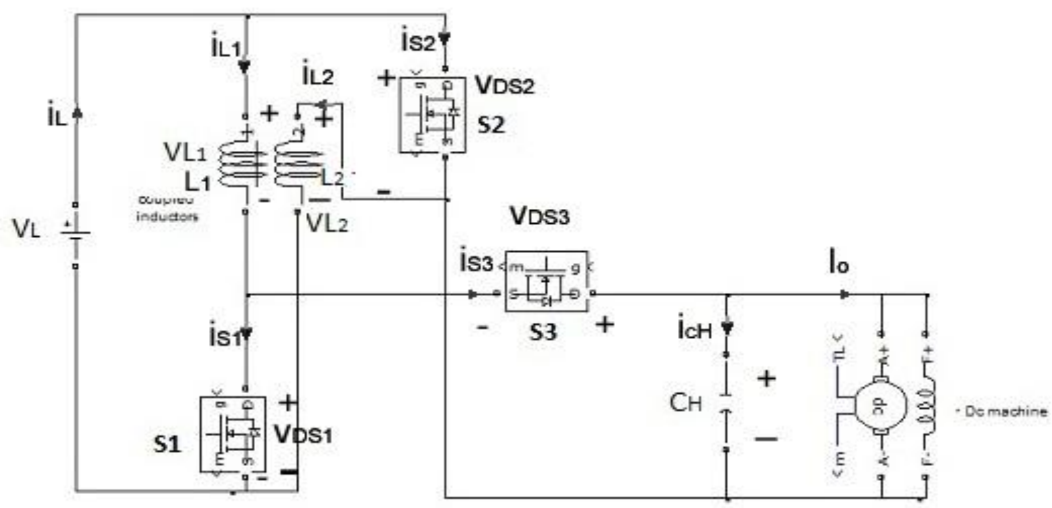

Fig4 step up mode

Fig 5: Some typical waveforms of the proposed converter in step-up mode (a) CCM operation (b) DCM operation (c) Mode 3 for DCM Mode

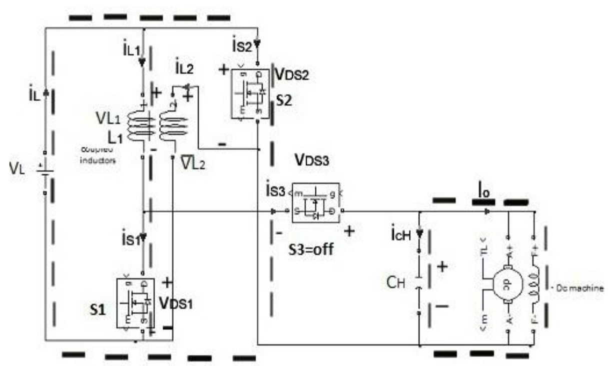

Fig (a)

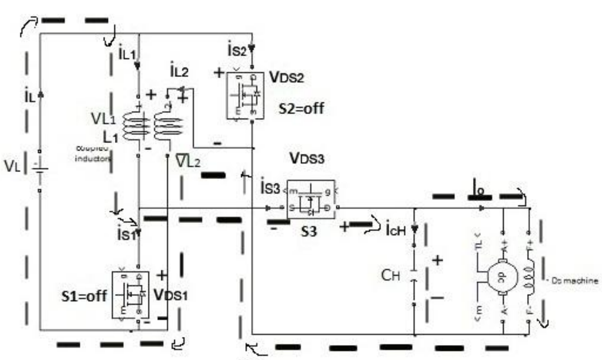

fig b

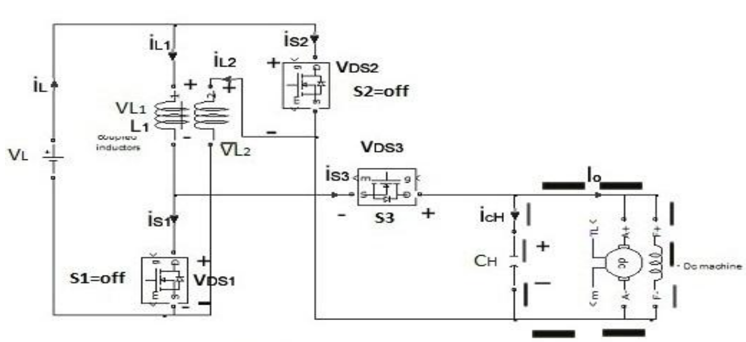

fig (c)

2.2 DCM Operation

Mode 1: During this time interval, S_1 and S_2 are turned on and $S3$ is turned off. The current flow path is shown in Fig. 5(a) The operating principle is same as that for the mode 1 of CCM operation

$$I_{L1p} = I_{L2p} = \frac{V_L D T_s}{(1+k)L} \tag{33}$$

Mode 2: During this time interval, S_1 and S_2 are turned off and $S3$ is turned on. The current flow path is shown in Fig 5 (b). The low-voltage side V_L and the coupled inductor are in series to transfer their energies to the capacitor C_H and the load. Meanwhile, the primary and secondary windings of the coupled inductor are in series. The currents iL_1 and iL_2 through the primary and secondary windings of the coupled inductor are decreased to zero at $t = t_2$. From eqn, another expression of IL_{1p} and IL_{2p} is given by

$$I_{L1p} = I_{L2p} = \frac{(V_H - V_L) D_2 T_s}{2(1+k)L} \tag{34}$$

Mode 3: During this $S1$ and $S2$ are still turned off and $S3$ is still turned on. The current flow path is shown in Fig 5(c). The energy stored in the coupled inductor is zero. Thus, $iL1$ and $iL2$ are equal to zero. The energy stored in the capacitor CH is discharged to the load. From above equation, is derived as follows

$$D_2 = \frac{2DV_L}{V_H - V_L} \tag{35}$$

From Fig, the average value of the output capacitor current during each switching period is given by

$$I_{cH} = \frac{\frac{1}{2} D_2 T_s I_{L1p} - I_o T_s}{T_s} = \frac{1}{2} D_2 I_{L1p} - I_o \tag{36}$$

By substituting above values we get

$$I_{cH} = \frac{D^2 V_L^2 T_s}{(1+k)L(V_H - V_L)} - \frac{V_H}{R_H} \tag{37}$$

Since IcH is equal to zero under steady state, above equations can be rewritten as follows:

$$\frac{D^2 V_L^2 T_s}{(1+k)L(V_H - V_L)} = \frac{V_H}{R_H} \tag{38}$$

Then, the normalized inductor time constant is defined as

$$T_{LH} \equiv \frac{L}{R_H T_s} = \frac{L f_s}{R_H} \tag{39}$$

where fs is the switching frequency. Substituting above equations we get, the voltage gain is given by

$$G_{DCM(step-up)} = \frac{V_H}{V_L} = \frac{1}{2} + \sqrt{\frac{1}{4} + \frac{D^2}{(1+k)\tau_{LH}}} \tag{40}$$

2.3 Boundary Operating Condition of CCM and DCM

When the proposed converter in step-up mode is operated in boundary conduction mode (BCM), the voltage gain of CCM operation is equal to the voltage gain of DCM operation. From above equations , the boundary normalized inductor time constant $\tau LH,B$ can be derived as follows

$$\tau_{LH,B} = \frac{D(1-D)^2}{2(1+k)(1+d)} \tag{41}$$

The curve of τ LH,B is plotted in Fig. If τLH is larger than τLH,B, the proposed converter in step-up mode is operated in CCM.

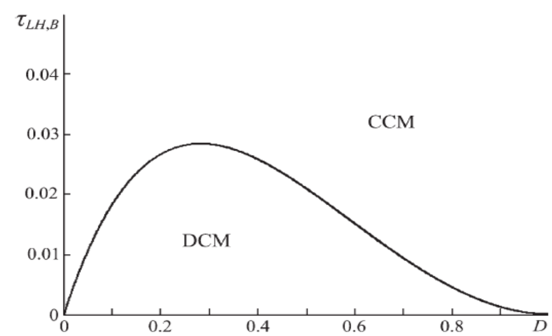

Fig-6 Boundary condition of the proposed converter in step-up mode (assuming $k = 1$)

III. STEP-DOWN MODE

The proposed converter in step-down mode of operation, the PWM technique is used to control the switch S_3. The switches S_1 and S_2 are the synchronous rectifiers

3.1 CCM Operation

Mode 1: During this time interval, S_3 is turned on and S_1/S_2 are turned off. The current flow path is shown in Fig 8(a). The energy of the high-voltage side V_H is transferred to the coupled inductor, the capacitor C_L, and the load.

$$i_{L1} = i_{L2}$$

$$u_{L1} + u_{L2} = V_H - V_L \tag{42}$$

By substituting we get

$$\frac{di_{L1}(t)}{dt} = \frac{di_{L2}(t)}{dt} = \frac{V_H - V_L}{2(1+k)L} \quad (43)$$

Mode 2: During this S_3 is turned off and S_1/S_2 are turned on. The current flow path is shown in Fig 8(b). The energy stored in the coupled inductor is released to the capacitor *CL* and the load.

Thus, the voltages across *L*1 and *L*2 are derived as

$$u_{L1} = u_{L2} = -V_L \quad (44)$$

By substituting we get

$$\frac{di_{L1}(t)}{dt} = \frac{di_{L2}(t)}{dt} = -\frac{V_L}{(1+k)L} \quad (45)$$

By using the state space averaging method, the following equation is obtained from

$$\frac{D(V_H - V_L)}{2(1+k)L} - \frac{(1-D)V_L}{(1+k)L} = 0 \quad (46)$$

By simplifying we get

$$G_{CCM(step-down)} = \frac{V_L}{V_H} = \frac{D}{2-D} \quad (47)$$

3.2 DCM Operation:

Mode 1: During this time interval, S_3 is turned on and S_1/S_2 are turned off. The current flow path is shown in Fig 8(a). The operating principle is same as that for the mode 1 of CCM operation. From, the two peak currents through the primary and secondary windings of the coupled inductor are given by

$$I_{L1p} = I_{L2p} = \frac{(V_H - V_L)DT_s}{2(1+k)L} \quad (48)$$

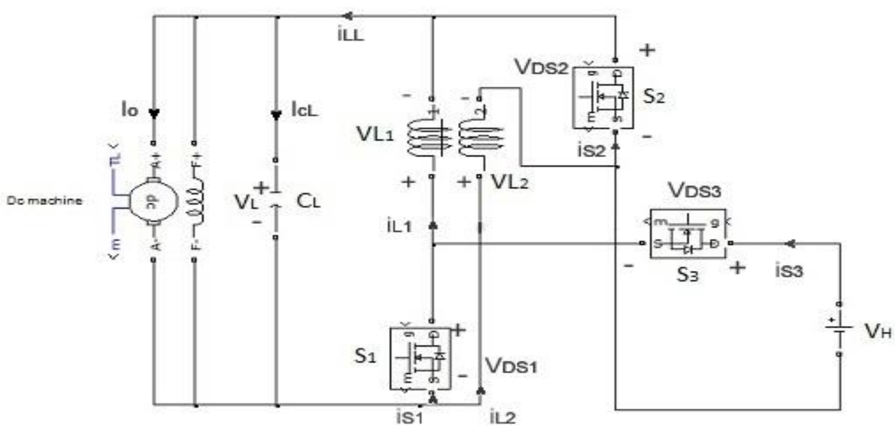

Fig 7 Step-down mode

Fig 8 Current flow path of the proposed converter in step-down mode. (a) Mode 1. (b) Mode 2. (c) Mode 3 for DCM operation

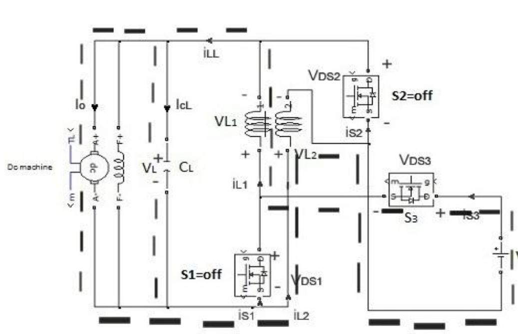

fig (a)

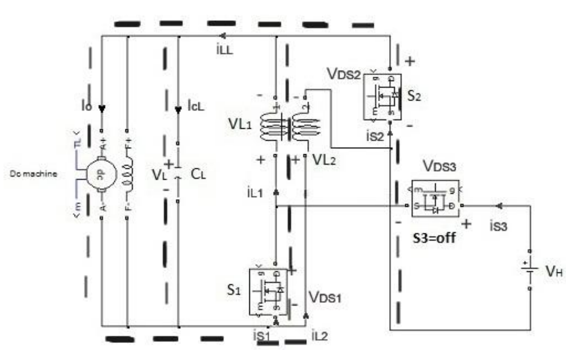

fig (b)

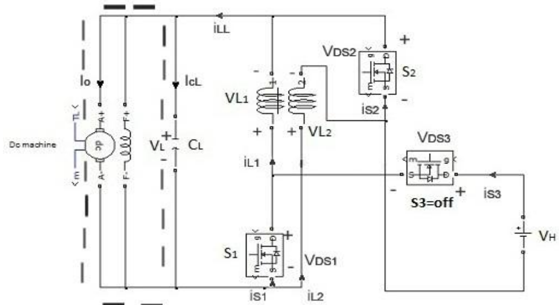

fig (c)

Mode 2*:* During this S_3 is turned off and S_1/S_2 are turned on. The current flow path is shown in Fig 8(b). The energy stored in the coupled inductor is released to the capacitor C_L and the load. The currents i_{L1} and $iL2$ through the primary and secondary windings of the coupled inductor are decreased to zero at $t = t_2$. From, another expression of IL_{1p} and IL_{2p} is given as

$$I_{L1p} = I_{L2p} = \frac{V_L D_2 T_s}{(1+k)L} \qquad (49)$$

Mode 3: During this time interval, S_3 is still turned off and S_1/S_2 are still turned on. The current flow path is shown in Fig 8(c). The energy stored in the coupled inductor is zero. Thus, i_{L1} and i_{L2} are equal to zero. The energy stored in the capacitor C_L is discharged to the load.

$$D_2 = \frac{D(V_H - V_L)}{2V_L} \qquad (50)$$

The average value of the output capacitor current during each switching period is given by

$$I_{cL} = \frac{\frac{1}{2}DT_s I_{L1p} + \frac{1}{2}D_2 T_s (2I_{L1p}) - I_o T_s}{T_s} = \frac{1}{2}DI_{L1p} + D_2 I_{L1p} - I_o \qquad (51)$$

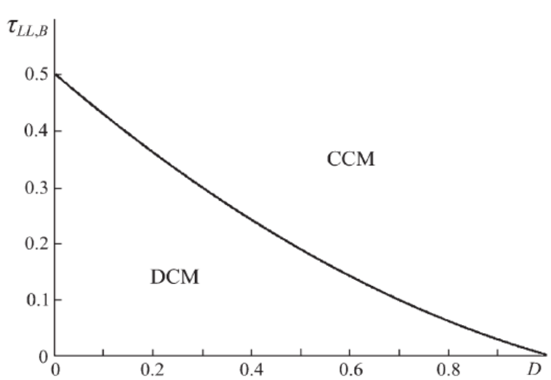

Fig 9 Boundary condition of the proposed converter in step-down mode

By substituting we get

$$\frac{D^2 T_s[(V_H - V_L)V_L + (V_H - V_L)^2]}{4(1+k)LV_L} = \frac{V_L}{R_L} \qquad (52)$$

$$G_{DCM(step-down)} = \frac{V_L}{V_H} = \frac{2}{1 + \sqrt{1 + \frac{16(1+k)\tau_{LL}}{D^2}}} \qquad (53)$$

3.3 Boundary Operating Condition of CCM and DCM

When the proposed converter in step-down mode is operated in BCM, the voltage gain of CCM operation is equal to the voltage gain of DCM operation, the boundary normalized inductor time constant $\tau LL, B$ can be derived as follows

$$\tau_{LL,B} = \frac{(1-D)(2-D)}{2(1+k)} \qquad (54)$$

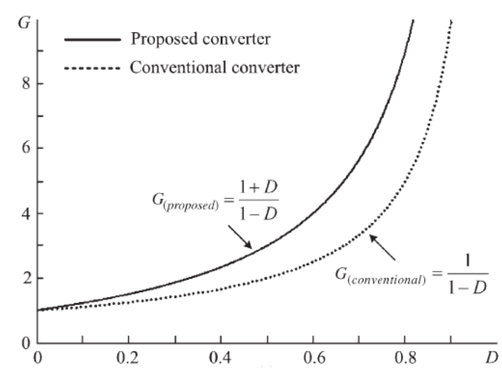

. (a)

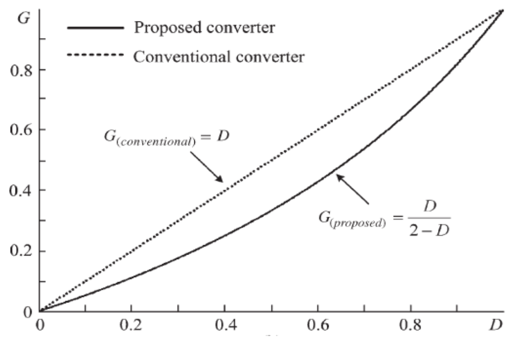

(b)

Fig 10 Voltage gain of the proposed converter and conventional bidirectional boost/buck converter in CCM operation in (a) Step-up mode (b) Step-down mode

IV RESULTS

In order to verify the performance of the proposed converter, a 70/210-V simulation circuit is built in the MATLAB / Simulink for the hybrid electric system. The electric specifications and circuit components are selected as V_L = 70 V, V_H = 210 V, f_s = 50 kHz, Po = 200 W, C_L = C_H = 330 μF, L_1 = L_2 = 15.5 μH ($rL1$ = rL_2 = 11 mΩ). Also, MOSFET IRF3710 ($VDSS$ = 100 V, $RDS(ON)$ = 23 mΩ, and ID = 57 A) is selected for S_1, S_2, and S_3. Some results in step-up and step-down modes are shows the waveforms of load voltage fig 11 and fig 14 and the DC machine performance characteristics waveforms in fig 12 and fig 15.and the input current i_L and the coupled inductor currents i_{L_1} and i_{L_2} in fig 13 for step-up mode. It can be seen that i_{L_1} is equal to i_{L_2}. The current i_L is double of the level of the coupled-inductor current during S_1/S_2 ON-period and equals the coupled-inductor current during S_1/S_2 OFF-period. Fig. 16 shows the waveforms of the current i_{LL} and the coupled-inductor currents i_{L_1} and i_{L_2} in step-down mode. It can be observed that i_{L_1} is equal to i_{L_2}. The current i_{LL} equals to the coupled-inductor current during S_3 ON-period and is double of the level of the coupled-inductor current during S_3 OFF-period.

Moreover, the prototype circuit of the conventional bidirectional boost/buck converter is also implemented in the laboratory. The electric specifications and circuit components are selected as VL = 14V, VH = 42V, fs = 50kHz, Po = 200 W, $L1$ = 28 μH ($rL1$ = 15 mΩ), CL = CH = 330 μF. At full-load condition, the measured efficiency of the proposed converter is 92.7% in step-up mode and is 93.7% in step-down mode. Also, the measured efficiency of the proposed converter is around 92.7%–96.2% in step-up mode and is around 93.7%–96.7% in step-down mode

Step-up mode:

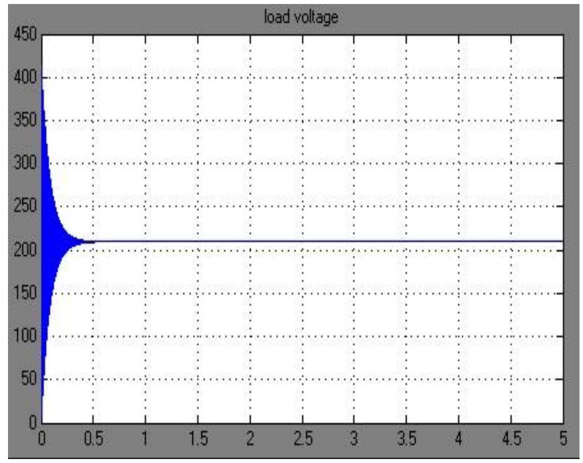

Fig 11 load voltage for step up mode

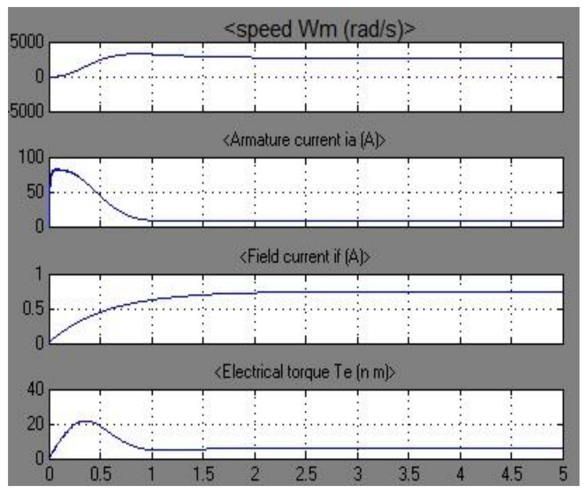

Fig 12 DC machine performance characteristics

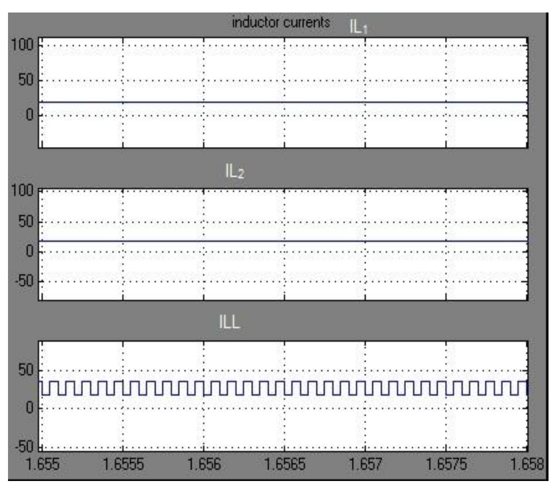

Fig 13 Inductor currents

Step-down mode:

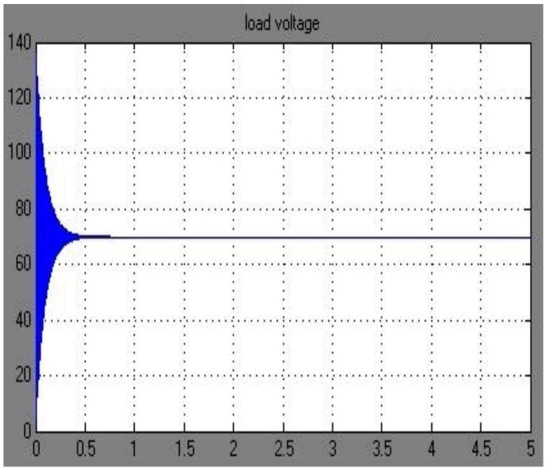

Fig 14 load voltage for step up mode

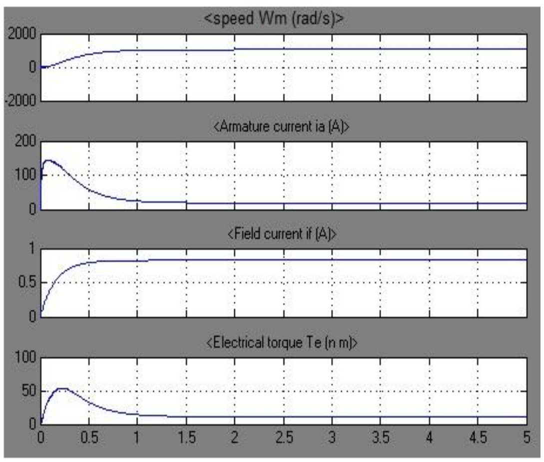

Fig 15 DC machine performance characteristics

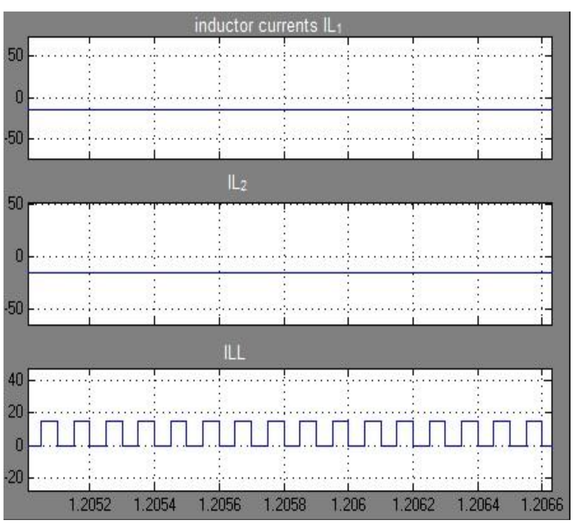

Fig 16 inductor currents

V CONCLUSION

This paper researches a novel bidirectional dc–dc converter drive. The circuit configuration of the proposed converter is very simple. The proposed converter has higher step-up and step-down voltage gains and lower average value of the switch current than the conventional bidirectional boost/buck converter which drives the hybrid vehicle. From the simulation results, it is see that the waveforms agree with the operating principle and steady-state analysis. At full-load condition, the measured efficiency is 92.7% in stepup mode and is 93.7% in step-down mode. Also, the measured efficiency is around 92.7%–96.2% in step-up mode and is around 93.7%–96.7% in step-down mode, which are higher than the conventional bidirectional boost/buck converter drive.

VI REFERENCES

[1] M. B. Camara, H. Gualous, F. Gustin, A. Berthon, and B. Dakyo, "DC/DC converter design for supercapacitor and battery power management in hybrid vehicle applications—Polynomial control strategy," IEEE Trans. Ind. Electron., vol. 57, no. 2, pp. 587–597, Feb. 2010.

[2] T. Bhattacharya, V. S. Giri, K. Mathew, and L. Umanand, "Multiphase bidirectional flyback converter topology for hybrid electric vehicles," IEEE Trans. Ind. Electron., vol. 56, no. 1, pp. 78–84, Jan. 2009.

[3] Z. Amjadi and S. S. Williamson, "A novel control technique for a switched-capacitor-converter-based hybrid electric vehicle energy storage system," IEEE Trans. Ind. Electron., vol. 57, no. 3, pp. 926–934,Mar. 2010.

[4] F. Z. Peng, F. Zhang, and Z. Qian, "A magnetic-less dc–dc converter for dual-voltage automotive systems," IEEE Trans. Ind. Appl., vol. 39, no. 2, pp. 511–518, Mar./Apr. 2003.

[5] A. Nasiri, Z. Nie, S. B. Bekiarov, and A. Emadi, "An on-line UPS system with power factor correction and electric isolation using BIFRED converter," IEEE Trans. Ind. Electron., vol. 55, no. 2, pp. 722–730, Feb. 2008.

[6] L. Schuch, C. Rech, H. L. Hey, H. A. Grundling, H. Pinheiro, and J. R. Pinheiro, "Analysis and design of a new high-efficiency bidirectional integrated ZVT PWM converter for DC-bus and battery-bank interface,"IEEE Trans. Ind. Appl., vol. 42, no. 5, pp. 1321–1332, Sep./Oct. 2006.

[7] X. Zhu, X. Li, G. Shen, and D. Xu, "Design of the dynamic power compensation for PEMFC distributed power system," IEEE Trans. Ind. Electron., vol. 57, no. 6, pp. 1935–1944, Jun. 2010.

[8] G. Ma, W. Qu, G. Yu, Y. Liu, N. Liang, and W. Li, "A zero-voltageswitching bidirectional dc–dc converter with state analysis and softswitching-oriented design consideration," IEEE Trans. Ind. Electron., vol. 56, no. 6, pp. 2174–2184, Jun. 2009.
[9] F. Z. Peng, H. Li, G. J. Su, and J. S. Lawler, "A new ZVS bidirectional dc–dc converter for fuel cell and battery application," IEEE Trans. Power Electron., vol. 19, no. 1, pp. 54–65, Jan. 2004.
[10] K. Jin, M. Yang, X. Ruan, and M. Xu, "Three-level bidirectional converter for fuel-cell/battery hybrid power system," IEEE Trans. Ind. Electron., vol. 57, no. 6, pp. 1976–1986, Jun. 2010.
[11] R. Gules, J. D. P. Pacheco, H. L. Hey, and J. Imhoff, "A maximum power point tracking system with parallel connection for PV stand-alone applications," IEEE Trans. Ind. Electron., vol. 55, no. 7, pp. 2674–2683, Jul. 2008.
[12] Z. Liao and X. Ruan, "A novel power management control strategy for stand-alone photovoltaic power system," in Proc. IEEE IPEMC, 2009, pp. 445–449.
[13] S. Inoue and H. Akagi, "A bidirectional dc–dc converter for an energy storage system with galvanic isolation," IEEE Trans. Power Electron., vol. 22, no. 6, pp. 2299–2306, Nov. 2007.
[14] L. R. Chen, N. Y. Chu, C. S. Wang, and R. H. Liang, "Design of a reflexbased bidirectional converter with the energy recovery function," IEEE Trans. Ind. Electron., vol. 55, no. 8, pp. 3022–3029, Aug. 2008.
[15] S. Y. Lee, G. Pfaelzer, and J. D.Wyk, "Comparison of different designs of a 42-V/14-V dc/dc converter regarding losses and thermal aspects," IEEE Trans. Ind. Appl., vol. 43, no. 2, pp. 520–530, Mar./Apr. 2007.
[16] Wensong Yu, Hao Qian, Jih-Sheng Lai "Design of High-Efficiency Bidirectional DC-DC Converter and High-Precision Efficiency Measurement"IEEE conf on power electronics pp-685-690 2008 july
[17] W. C. Liao T. J. Liang H. H. Liang H. K. Liao *L. S. Yang **K.C. Juang J. F. Chen" Study and Implementation of a Novel Bidirectional DC-DC Converter with High Conversion Ratio" IEEE conf on power electronics pp-134-140. jan 2011
[18] Rou-Yong Duan1 and Jeng-Dao Lee" Soft Switching Bidirectional DC-DC Converter with Coupled Inductor" IEEE conf on power electronics pp-2797-2802. jan 2011
[19] R.-Y. Duan, J.-D. Lee" High-efficiency bidirectional DC-DC converter with coupled inductor" Published in IET Power Electronics

Received on 21st December 2010 Revised on 31st March 2011

Author Profile

N. Mahesh received B.Tech from Lakireddy Balireddy College of engineering, India in 2010. Presently he is pursuing M.Tech in KL University. His areas of interests are power electronics, DC Machines and networks theory.

D.Seshi Reddy, received B.E and M.Tech from Andhra University college of engineering and National Institute of Technology Calicut, India in 2002 And 2004, respectively. Presently he is pursuing Ph.D from JNT university, hyderabad. Since 2007, he has been with the department of electrical and electronics engineering, KL University, where he is currently an associate professor. He has published more than ten journals and conferences recent trends in power system. His current research interests include measurement of power quality problems, Flexible AC transmission systems.